Table 2. Oligonucleotide primer pairs.

Name	Oligonucleotide primer pair sequences
o1	5′-TTTCTTTTCACCTGCTCTGGCTATAATTATAATTGGTTACTTAAAAATGCACCGTTAAGAACCATATCCAAGAATCAAAATTTTTTGTTCTTTTTTTTTGA-3′ and 5′-TCTTAACGGTGCATTTTTAAGGGTAATAACTGATATAATT-3′
o2	5′-TCGTACGTTCCTTCTAGGTTTTGCACGCACTATCTGAGGCGTTATAGGTTCAATTTGGTAATTAAAGATAGAGTTGTTTTTTGTTCTTTTTTTTTGA-3′ and 5′-TACCAAATTGAACCTATAACGGGTAATAACTGATATAATT-3′
o3	5′-TTTATATTTCTTGACCATCCTTTACACAAAGTCTATAGATCCACTGGAAAGCTTCGTGGGCGTAAGAAGGCAATCTATTATTTTTTGTTCTTTTTTTTGA-3′ and 5′-GGGCCTCGATTCCCGAACTAGGGTAATAACTGATATAATT-3′
o4	5′-AATTATATCAGTTATTACCCTTAAAAATGCACCGTTAAGAACCATATCCAAGAATCAAAATTTACGGCTTTGAAAAAGTAATTTCGTGACCTTC-3′ and 5′-AAGATTAACTGTATATTATTGCCTGAGAGTTCTAGATCATG-3′
o5	5′-AATTATATCAGTTATAGGTTCAATTTGGTAATTAAAGATAGAGTTGTAAGTTTCATTGAGAGTCTTACTCATCTTCAGGTACAATTGCAC-3′ and 5′-AAAAAAAAGTTTTCAGACGGACTTAAACCGCCAACCAGCC-3′
o6	5′-AATTATATCAGTTATTACCCCCACTGGAAAGCTTCGTGGGCGTAAGAAGGCAATCTATTATAGTTCGGGAATCGAGGCCCGTATTTCGAGGCTTTTGCTT-3′ and 5′-GCATATATGACGAGATTTAATTATCGCCAATAGGTTCTTT-3′
o7	5′-TTTCTTTTCACCTGCTCTGGCTATAATTATAATTGGTTACTTAAAAATGCACCGTTAAGAACCATATCCAAGAATCAAAATTTTTTGTTCTTTTTTTTGA-3′ and 5′-AAGATTAACTGTATATTATTGCCTGAGAGTTCTAGATCATG-3′
o8	5′-TCGTACGTTCCTTCTAGGTTTTGCACGCACTATCTGAGGCGTTATAGGTTCAATTTGGTAATTAAAGATAGAGTTGTAAGTTTCATTGAGAGTCTTACTCATCTTCAGGTACAATTGCAC-3′ and 5′-AAAAAAAAGTTTTCAGACGGACTTAAACCGCCAACCAGCC-3′
o9	5′-TTTATATTTCTTGACCATCCTTTACACAAAGTCTATAGATCCACTGGAAAGCTTCGTGGGCGTAAGAAGGCAATCTATTATTTTTTGTTCTTTTTTTTGA-3′ and 5′-GCATATATGACGAGATTTAATTATCGCCAATAGGTTCTTT-3′
o10	5′-TTTTGCTAGCATGGAGCCCCTGTTCCCAGC-3′ and 5′-TTGGAGATCTTCACAGCTTGCTGGTCTGCA-3′
o11	5′-CCCGACGTCCACGGACTATAGACTATACTA-3′ and 5′-CCTGACGTCTGAACCAGTCCTAAAACGAGT-3′
o12	5′-TTTTGGATCCGTGAGCAAGGGCGAGGAGCT-3′ and 5′-GGGGAGATCTTTACTTGTACAGCTCGTCCA-3′.
o13	5′-TTTTGCTAGCATGGAGCCCCTGTTCCCAGC-3′ and 5′-GGGAAGATCTCAGCTTGCTGGTCTGCATAA-3′
o14	5′-GGGGGCTAGCATGAGATTTCCTTCAATTTT-3′ and 5′-TGGGAACAGGGGCTCTCTTTATCCAAAGA-3′
o15	5′-TCTTTGGATAAAAGAGAGCCCCTGTTCCCA-3′ and 5′-TTGGAGATCTTCACAGCTTGCTGGTCTGCA-3′
o16	5′-GGGGGCTAGCATGAGATTTCCTTCAATTTT-3′ and 5′TTGGAGATCTTCACAGCTTGCTGGTCTGCA-3′.
o17	5′-TTTTGCTAGCATGAGATTTCCTTCAATTTTTACTGCAGTTTTATTCGCAGCATCCTCCGCATTAGCTGAGCCCCTGTTCCCAGCCTCCACGCCCAGC-3′ and 5′-GGGAAGATCTCAGCTTGCTGGTCTGCATAA-3′
o18	5′-AAAAGCTAGCATGTCTGATGCGGCTCCTTCATTGAGCAATCTATTTTATGATCCAACGTATAAATCCTGGTGAGCCCCTGTTCCCAGCCTCCACGCCCAGC-3′ and 5′-GGGAAGATCTCAGCTTGCTGGTCTGCATAA-3′
o19	5′-TTTTGCTAGCATGGAGCCCCTGTTCCCAGC-3′ and 5′-TTGGAGATCTTCAAGCGTAATCTGGAACATCGTATGGGTACAGCTTGCTGGTCTGCA-3′
o20	5′-GGGGGCTAGCATGAGATTTCCTTCAATTTT-3′ and 5′-TTGGAGATCTTCAAGCGTAATCTGGAACATCGTATGGGTACAGCTTGCTGGTCTGCA-3′
o21	5′-TTTTGCTAGCATGAGATTTCCTTCAATTTTTACTGCAGTTTTATTCGCAGCATCCTCCGCATTAGCTGAGCCCCTGTTCCCAGCCTCCACGCCCAGC-3′ and 5′-TTGGAGATCTTCAAGCGTAATCTGGAACATCGTATGGGTACAGCTTGCTGGTCTGCA-3′
o22	5′-AAAAGCTAGCATGTCTGATGCGGCTCCTTCATTGAGCAATCTATTTTATGATCCAACGTATAAATCCTGGTGAGCCCCTGTTCCCAGCCTCCACGCCCAGC-3′ and 5′-TTGGAGATCTTCAAGCGTAATCTGGAACATCGTATGGGTACAGCTTGCTGGTCTGCA-3′
o23	5′-TTTTGGATCCATGGTGAGCAAGGGCGAGGA-3′ and 5′-AAAACCGCGGTTACTTGTACAGCTCGTCCA-3′
o24	5′-CCCCCCGCGGGAAATAAATTGAATT-3′ and 5′-TTTTGAGCTCAGCTTTAACGAACGCAGAAT-3′
o25	5′-GAAACTCGAGATCACCCTGCATTGCCTCTT-3′ and 5′-CCCGGATCCTTTTTTTTTTTTTTTGT-3′
o26	5′-GGGGCTCGAGTCATACTTAGAAAAAACATGT-3′ and 5′GGGGAGATCTTCATATAATACCAATTTTTT-3′
o27	5′-GGGGCTCGAGTCATACTTAGAAAAAACATGT-3′ and 5′-CCCCAGATCTTCAGTACAAACCACATTCTTTAAGGTTTTGCTGGATGATTAGATCGGTGACTGCACTCAA-3′

Table 3. PCR-amplified DNA fragments used for yeast gene disruptions and plasmid constructions.

Amplified DNA fragments	Relevant genetic descriptions	Template DNAs	Primer pairs
5′STE2-URA3	80-bp *STE2-5′* flanking region and *URA3*	pRS406	1
5′SST2- URA3	80-bp *SST2-5′* flanking region and *URA3*	pRS406	2
5′FAR1- URA3	80-bp *FAR1-5′* flanking region and *URA3*	pRS406	3
hrSTE2-3′STE2	40-bp *STE2-5′* flanking region and 1-kbp *STE2-3′* flanking region	BY4741 genomic DNA	4
hrSST2-3′SST2	40-bp *SST2-5′* flanking region and 1-kbp *SST2-3′* flanking region	BY4741 genomic DNA	5
hrFAR1-3′FAR1	40-bp *FAR1-5′* flanking region and 1-kbp *FAR1-3′* flanking region	BY4741 genomic DNA	6
5′STE2-URA3-hrSTE2-3′STE2	*5′STE2- URA3* and *hrSTE2-3′STE2*	*5′STE2-URA3* and *hrSTE2-3′STE2*	7
5′SST2-URA3-hrSST2-3′SST2	*5′SST2-URA3* and *hrSST2-3′SST2*	*5′SST2-URA3* and *hrSST2-3′SST2*	8
5′FAR1-URA3-hrFAR1-3′FAR1	*5′FAR1-URA3* and *hrFAR1-3′FAR1*	*5′FAR1-URA3* and *hrFAR1-3′FAR1*	9
SSTR5-HA	The *SSTR5-HA* fragment in pBlue-SSTR5-HA	Human brain cDNA (Invitrogen, Carlsbad, CA, USA)	10
2μ origin	The *Aat*II 2μ origin fragment in pRS401+2 μm	pWI3	11
ECFP	The *Bam*HI-*Bgl*II *ECFP* fragment in pGK421-ECFP	pECFP-C1	12
SSTR5	The *Nhe*I-*Bgl*II *SSTR5* fragment in pSSTR5-CF2	pBlue-SSTR5-HA	13
Prepro-α-factor	Template DNA of overlap PCR for the *prepro-SSTR5* amplification	pWI3α	14
hr-SSTR5	Template DNA of overlap PCR for the *prepro-SSTR5* amplification	pBlue-SSTR5-HA	15
Prepro-SSTR5	The *Nhe*I-*Bam*HI *prepro-SSTR5* fragment in pSSTR5-CF2alpha	*prepro-α-factor and hr-SSTR5*	16
Pre-SSTR5	The *Nhe*I-*Bgl*II *pre-SSTR5* fragment in pSSTR5-CF2al	pBlue-SSTR5-HA	17
Ste2N-SSTR5	The *Nhe*I-*Bgl*II *Ste2N-SSTR5* fragment in pSSTR5-CF2st	pBlue-SSTR5-HA	18
SSTR5-HA	The *Nhe*I-*Bgl*II *SSTR5-HA* fragment in pGK-SSTR5-HA	pBlue-SSTR5-HA	19
Prepro-SSTR5-HA	The *Nhe*I-*Bgl*II *prepro-SSTR5-HA* fragment in pGKalpha-SSTR5-HA	pBlue-SSTR5-HA	20
Pre-SSTR5-HA	The *Nhe*I-*Bgl*II *pre-SSTR5-HA* fragment in pGKal-SSTR5-HA	pBlue-SSTR5-HA	21
STE2N-SSTR5-HA	The *Nhe*I-*Bgl*II *STE2N-SSTR5-HA* fragment in pGKst-SSTR5-HA	pBlue-SSTR5-HA	22
EGFP	The *Bam*HI-*Sac*II *EGFP* fragment in pMHG-FIG1	pEGFP-C1	23
PGK3′	The *Sac*II-*Sac*I *PGK3′* fragment in pMHG-FIG1	pTA2-PGK	24
5′FIG1	The *Xho*I-*Bam*HI 450-bp *FIG1-5′* flanking region in pMHG-FIG1	BY4741 genomic DNA	25
5′GPA1 -GPA1	The *Xho*I-*Bgl*II 1-kp *GPA1-5′* flanking region–*GPA1* in pSL-GPA1	BY4741 genomic DNA	26
5′GPA1-Gi3tp	The *Xho*I-*Bgl*II 1-kb *GPA1-5′* flanking region–*Gi3tp* in pSL-Gi3tp	BY4741 genomic DNA	27

suggesting that introduction of SS improves ligand sensitivity (Fig. 2B and Table 5).

Estimation of expression levels and observation of localization of CFP fluorescent-tagged SSTR5 receptors with or without introduction of SS in yeast

To estimate expression levels and observe the subcellular localizations of the SSTR5 receptors with or without addition of SS in yeast, the CFP fluorescent tag protein was introduced at the carboxyl-terminus of the natural SSTR5 and the engineered SS-introduced SSTR5 receptors (SSTR5-CFP and three types of SS-SSTR5-CFPs) were expressed in the yeasts. Figure 3 shows the average intensities of CFP fluorescence of 10,000 cells normalized with the control strain harbouring mock vector. Compared with the SSTR5-CFP-expressing cells without addition of SS, the yeast cells expressing the all three types of SS-SSTR5-CFPs displayed higher fluorescence intensities in the following order: SSTR5-CFP < prepro-SSTR5-CFP < pre-SSTR5-CFP <Ste2N -SSTR5-CFP. The result suggests that introduction of SS accelerates SSTR5 receptor expression levels in yeast cells and also corresponds to findings of previous reports (*12*, *15*).

To confirm the localizations of SSTR5 receptors in yeast, SSTR5-CFP-expressing cells were subsequently observed by fluorescence microscopy (Fig. 4). Among the four SSTR5-CFP receptors, the Ste2N-SSTR5-CFP receptor was localized to the plasma membranes. In the case of yeast cells expressing SSTR5-CFP without addition of SS, CFP fluorescence appeared to be mainly accumulated in vacuoles and was partially observed on the plasma membranes and inside the cells. On the other hand, the prepro-SSTR5-CFP receptor was predominantly localized to the endoplasmic reticulum and Golgi apparatus accompanied with strong CFP fluorescence in yeast cells. The pre-SSTR5-CFP receptor displayed an intermediate localization pattern between prepro-SSTR5-CFP and Ste2N-SSTR5-CFP.

Discussion

In this study, to guide the easy-to-use yeast-based system to comfortably screen primary drug candidates

Table 4. Plasmids.

Plasmid	Relevant genotype	Reference or source
pRS406	Containing *URA3* marker	American Type Culture Collection, Manassas, VA, USA
pBluescript II KS(+)	Cloning vector	Stratagene, La Jolla, CA, USA
pBlue-SSTR5-HA	*SSTR5-HA* in pBluescript II KS(+)	This study
pWI3	Containing 2μ origin	(*26*)
pRS401	Containing *MET15* marker	American Type Culture Collection, Manassas, VA, USA
pTA2-PGK	Containing multi cloning sites (*MCS*) between the yeast *PGK1* promoter (*PGK5'*) and *PGK1* terminator (*PGK3'*)	(*27*)
pRS401+2 μm	2μ origin in pRS401	This study
pGK421	The *XhoI-NheI PGK5'-MCS-PGK3'* digested from pTA2-PGK in pRS401+2 μm	This study
pECFP-C1	Containing *ECFP*	Clontech, BD Biosciences, Palo Alto, CA, USA
pGK421-ECFP	*ECFP* in pGK421	This study
pSSTR5-CF2	*SSTR5* in pGK421-ECFP	This study
pWI3α	Containing *prepro-α-factor*	(*26*)
pSSTR5-CF2alpha	*Prepro-SSTR5-ECFP* in pGK421	This study
pSSTR5-CF2al	*Pre-SSTR5-ECFP* in pGK421	This study
pSSTR5-CF2st	*STE2N-SSTR5-ECFP* in pGK421	This study
pGK-SSTR5-HA	*SSTR5-HA* in pGK421	This study
pGKalpha-SSTR5-HA	*Prepro-SSTR5-HA* in pGK421	This study
pGKal-SSTR5-HA	*Pre-SSTR5-HA* in pGK421	This study
pGKstSSTR5-HA	*STE2N-SSTR5-HA* in pGK421	This study
pEGFP-C1	Containing *EGFP*	Clontech, BD Biosciences, Palo Alto, CA, USA
pRS403 + 2 μm	Containing *HIS3* marker and 2μ origin	(*28*)
pMHG-FIG1	*5'FIG1-EGFP-PGK3'* in pRS403 + 2 μm	This study
pGK415	Containing *PGK5'-MCS-PGK3'*, *LEU2* marker and *CEN/ARS* origin	(*28*)
pSL-GPA1	*5'GPA1-GPA1-PGK3'* in pGK415	This study
pSL-Gi3tp	*5'GPA1-Gi3tp-PGK3'* in pGK415	This study

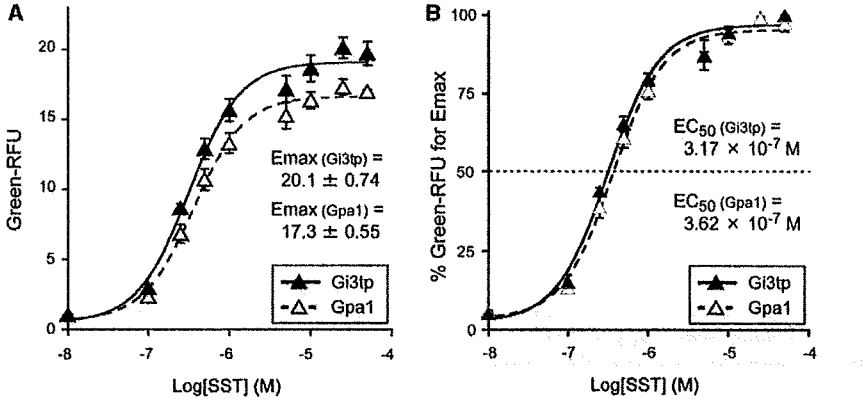

Fig. 1 Dose–response curves for SST-specific SSTR5 signalling activities of recombinant yeast cells expressing different types of intracellular peripheral G-protein α-subunits. As Gα-subunits for the functional SST-specific SSTR5 signalling, yeast endogenous Gpa1 and yeast–human chimeric Gi3tp were compared using the *GFP* reporter gene. The signalling activities of recombinant strains MI-170-1 (Gpa1, open symbol) and MI-170-2 (Gi3tp, closed symbol) were evaluated as described in 'MATERIALS AND METHODS' section. (**A**) Pharmacological efficacies of yeast transformants were represented by green-RFU normalized with the green fluorescent intensities of the SST-untreated yeast cells as the reference values, respectively. (**B**) Pharmacological potencies of yeast transformants were represented by relative green-RFU normalized with the values of maximal effects of SST-specific dose–responses as the reference values, respectively. Data points represent the mean of triplicate independent experiments and error bars represent the standard deviation. EC_{50} values were determined using KaleidaGraph4.0 fits to a dosersplgst model.

for human GPCRs, we aimed to control human SSTR5 signalling activity in yeast via addition of SS. We used yeast-based fluorescent assay systems for evaluation of SSTR5 signalling by the *GFP* reporter gene. SST-specific stimulation of human SSTR5 receptor can be converted into yeast pheromone signalling via the yeast endogenous Gα-subunit protein (Gpa1), and the resulting green fluorescent signals from the activated cells are quantitatively and immediately measurable by direct analysis of non-destructive cells using a flow cytometer.

The substitution of carboxyl-terminal 5 aa residues of the endogenous Gpa1 for the yeast Gpa1-human Gαi3 chimeric Gα-subunit protein, Gi3tp, was effective

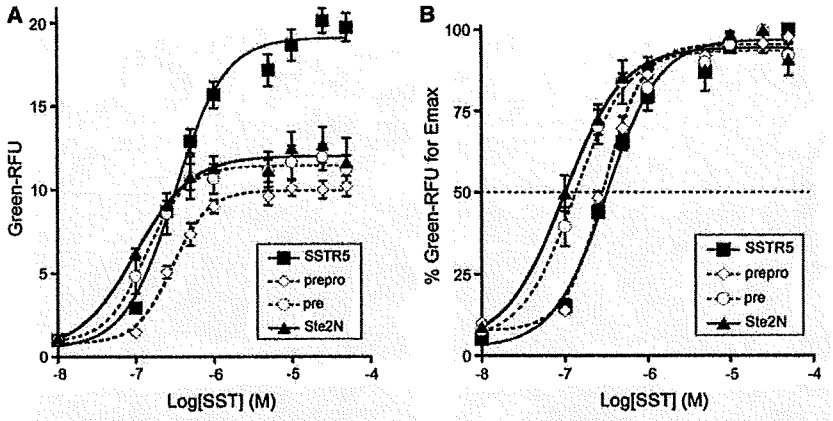

Fig. 2 Dose–response curves for SST-specific signalling activities of SSTR5 with or without additional SS in yeast cells. To examine the effects of SS for the SST-specific SSTR5 signalling, prepro-SSTR5, pre-SSTR5 and Ste2N-SSTR5 were prepared. The signalling activities of recombinant strains MI-170-3 (prepro), MI-170-4 (pre) and MI-170-5 (Ste2N) were evaluated using the *GFP* reporter gene as described in 'MATERIALS AND METHODS' section. **(A)** Pharmacological efficacies of yeast transformants were represented by green-RFU normalized with the green fluorescent intensities of the SST-untreated yeast cells as the reference values, respectively. **(B)** Pharmacological potencies of yeast transformants were represented by relative green-RFU normalized with the values of maximal effects of SST-specific dose responses as the reference values, respectively. MI-170-2 data shown in Fig. 1 are displayed for comparison. Data points represent the mean of triplicate independent experiments and error bars represent the standard deviation.

Table 5. Characterization of SSTR5 receptors with and without SS expressed in MI-170 yeast cells.

Receptor	Expression level[a]	Maximal effect[b]	EC_{50} value[c]
SSTR5	2.58 ± 0.54	20.1 ± 0.74	3.17×10^{-7}
Prepro-SSTR5	4.81 ± 0.99	10.2 ± 0.62	2.92×10^{-7}
Pre-SSTR5	6.12 ± 0.49	11.9 ± 0.76	1.37×10^{-7}
Ste2N-SSTR5	8.43 ± 1.37	12.7 ± 1.1	1.01×10^{-7}

[a]Expression levels cited the values in Fig. 3.
[b]Maximal effects cited the values in Fig. 2A.
[c]EC_{50} values cited the values in Fig. 2B.

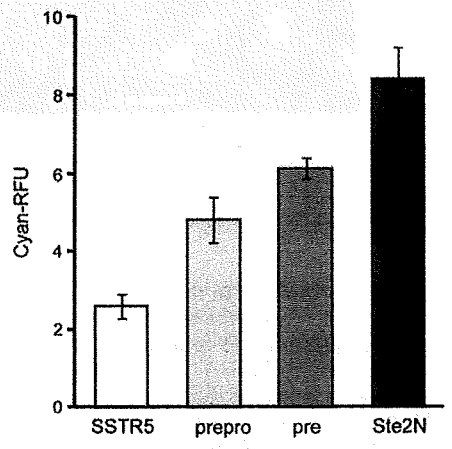

Fig. 3 Estimation of expression levels of CFP-fluorescent tagged SSTR5 receptors with or without additional SS sequences. Four CFP-fluorescent tagged SSTR5 constructs—SSTR5-CFP, prepro-SSTR5-CFP, pre-SSTR5-CFP and Ste2N-SSTR5-CFP—were prepared to generate recombinant strains MI-170-6 (SSTR5), MI-170-7 (prepro), MI-170-8 (pre) and MI-170-9 (Ste2N), respectively. Cellular cyan-RFU was calculated as described in 'MATERIALS AND METHODS' section. Data represent the mean of triplicate independent experiments and error bars represent the standard deviation.

to functionally couple the SSTR5 to the yeast pheromone signalling pathway as shown in a previous report (*19*). Obviously, the maximum effect responding to the highest concentration of SST was enhanced in the Gi3tp-expressing yeast cells and the dose–response curves exposed the suitable pharmacological potency and efficacy of Gi3tp for the SSTR5 (Fig. 1). Therefore, the SSTR5 Gα-subunit was successfully optimized by substitution of chimeric Gi3tp for endogenous Gpa1 in the yeast-based fluorescent signalling assay system. Although productivity and transportation of the heterogous GPCRs could be enhanced via introduction of the yeast SS in yeast cells (*12*, *15*, *16*), the signalling functions of SS-attached GPCRs have been rarely described. When constructing a superior ligand screening method using a yeast-based fluorescent signalling assay system, either higher sensitivity or a higher maximal effect should be achieved in the system, although it is difficult to simultaneously achieve both. Indeed, the signalling properties desired in yeast-based signalling assay systems differ depending on the aims for varied assay applications. For example, systems with high sensitivity are useful for the agonist detection assay at low concentrations or the competitive assay with antagonists; on the other hand, systems with high maximal effect are useful for the high-throughput ligand screening system by FACS. By controlling the signalling property, we could construct a suitable yeast-based assay system depending on the aims of the assays. Therefore, to control signalling ability of human SSTR5 in a yeast-based signalling assay system, we constructed four types of SSTR5 receptor variants and investigated their SST-specific signalling activities in yeast cells.

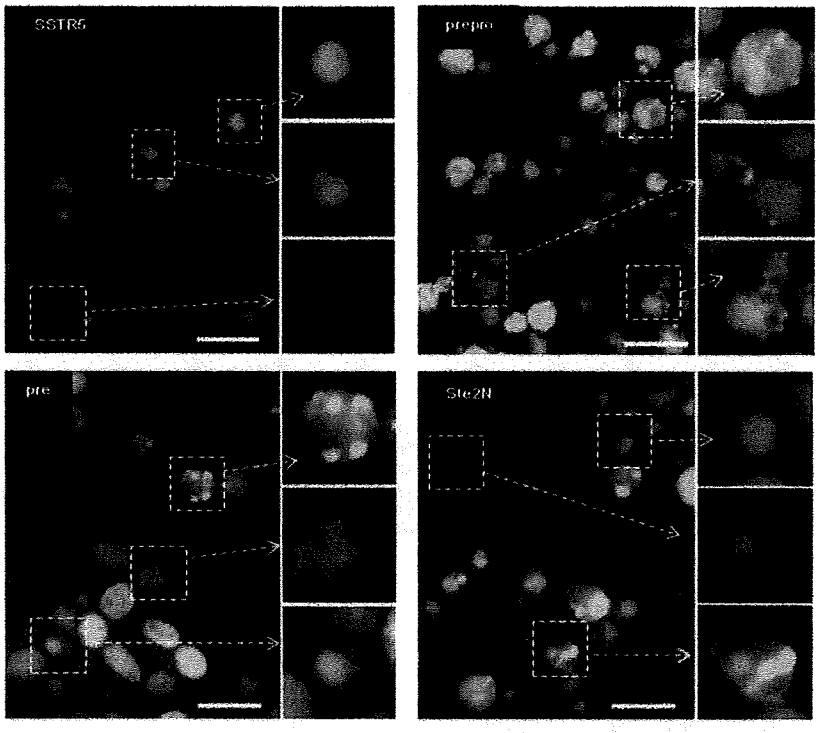

Fig. 4 Observation of localization patterns of CFP-fluorescent tagged SSTR5 receptors with or without additional SS. The yeast strain MI-170 was used as the host strain to introduce CFP-fluorescent tagged SSTR5 receptors without or with additional SS. Four CFP-fluorescent tagged SSTR5 constructs—SSTR5-CFP, prepro-SSTR5-CFP, pre-SSTR5-CFP and Ste2N-SSTR5-CFP—were prepared to generate recombinant strains MI-170-6 (SSTR5), MI-170-7 (prepro), MI-170-8 (pre) and MI-170-9 (Ste2N), respectively. The cellular cyan fluorescence was observed with the fluorescence microscope as described in 'MATERIALS AND METHODS' section. White bars represent 10 μm.

Insertions of any three SS to the amino-terminus of SSTR5 drastically decreased the efficacies of the engineered receptors expressing cells compared to that of the native SSTR5 form (Fig. 2A and Table 5). The pharmacological potencies of SST for the engineered SS-SSTR5 receptors were higher than that of the native form SSTR5 receptor; Ste2N-SSTR5 in particular displayed the highest potency for SST-dependent signalling activity (Fig. 2B and Table 5). Therefore, the Ste2N-SSTR5 receptor is useful for constructing high-sensitivity yeast-based assay systems such as agonist detection assays at low concentrations and competitive assays with antagonists.

FACS analysis of the CFP fusion proteins indicated that addition of SS increased SSTR5 expression levels in yeast cells (Fig. 3). However, not all of the CFP-tagged SSTR5 molecules were localized to the plasma membrane because the CFP-tagged SSTR5 molecules were transported by different protein sorting pathways depending on the SS properties (Fig. 4). These results suggest that the SS of the typical secretory protein is not suitable for functional expression of seven transmembrane SSTR5 receptors at the yeast plasma membrane. The potency was decreased in the case of prepro-SSTR5, which may be caused by the lower amount of the receptors on yeast cell surface.

The large amounts of SSTR5 receptors at the yeast plasma membrane accelerate the ligand binding even low concentration of SST, as a result, the potency of Ste2N-SSTR5 was improved. Although ligand binding ability seemed to effect on the efficacy, Sander *et al.* (*16*) reported the introduction of Ste2-derived SS to human D_{2s} dopamine receptor did not affect the ligand binding ability when the receptor was expressed on the yeast cell surface. Therefore, we assumed the binding ability of SS-attached SSTR5 is almost same as that of SSTR5. One of the possible explanations for decreased efficacy is that introduction of SS at amino-terminus may inhibit the receptor dimerization (*20*, *21*). Dimerization of GPCRs should be required for desensitization and internalization, which are necessary events to refresh ligand-bound receptors and regenerate ligand-free receptors at the plasma membrane for responding to the redundant extracellular ligands (*22*, *23*).

In conclusion, we demonstrated SST-specific signalling functions of SSTR5 via introduction of SSs in yeast. Using a yeast–human Gi3tp chimera, we optimized the yeast-based fluorescent assay system. Introduction of Ste2N to the amino-terminus of human SSTR5 significantly improved pharmaceutical potency in the yeast-based fluorescent assay system. This finding will be an informative support to

construct optimal yeast-based flow cytometric signalling assay systems using other human GPCRs and will be helpful for execution of primary drug screening.

Acknowledgements

The authors thank Prof. Shun'ichi Kuroda and Dr Kenji Tatematsu for their help.

Funding

This work was supported by a Grant-in-Aid for Scientific Research on Priority Areas (Life surveyor) and in part by a Special Coordination Funds for Promoting Science and Technology, Creation of Innovation Centres for Advanced Interdisciplinary Research Areas (Innovative Bioproduction Kobe) from the Ministry of Education, Culture, Sports, Science and Technology of Japan, and was funded in part by AS ONE Corporation.

Conflict of interest

None declared.

References

1. Wise, A., Gearing, K., and Rees, S. (2002) Target validation of G-protein coupled receptors. *Drug Discov. Today* **7**, 235–246
2. Reisine, T. and Bell, G. (1995) Molecular biology of somatostatin receptors. *Endocr. Rev.* **16**, 427–442
3. Shimon, I., Taylor, J.E., Dong, J.Z., Bitonte, R.A., Kim, S., Morgan, B., Coy, D.H., Culler, M.D., and Melmed, S. (1997) Somatostatin receptor subtype specificity in human fetal pituitary cultures. Differential role of SSTR2 and SSTR5 for growth hormone, thyroid-stimulating hormone, and prolactin regulation. *J. Clin. Invest.* **99**, 789–798
4. Casarini, A.P., Jallad, R.S., Pinto, E.M., Soares, I.C., Nonogaki, S., Giannella-Neto, D., Musolino, N.R., Alves, V.A., and Bronstein, M.D. (2009) Acromegaly: correlation between expression of somatostatin receptor subtypes and response to octreotide-lar treatment. *Pituitary* **12**, 297–303
5. Duran-Prado, M., Gahete, M.D., Martinez-Fuentes, A.J., Luque, R.M., Quintero, A., Webb, S.M., Benito-Lopez, P., Leal, A., Schulz, S., Gracia-Navarro, F., Malagon, M.M., and Castano, J.P. (2009) Identification and characterization of two novel truncated but functional isoforms of the somatostatin receptor subtype 5 differentially present in pituitary tumors. *J. Clin. Endocrinol. Metab.* **94**, 2634–2643
6. Vieira Neto, L., Taboada, G.F., and Gadelha, M.R. (2008) Somatostatin receptors subtypes 2 and 5, dopamine receptor type 2 expression and *gsp* status as predictors of octreotide LAR responsiveness in acromegaly. *Arq. Bras. Endocrinol. Metabol.* **52**, 1288–1295
7. Dowell, S.J. and Brown, A.J. (2002) Yeast assays for G-protein-coupled receptors. *Receptors Channels* **8**, 343–352
8. Ladds, G., Goddard, A., and Davey, J. (2005) Functional analysis of heterologous GPCR signalling pathways in yeast. *Trends Biotechnol.* **23**, 367–373
9. Klco, J.M., Nikiforovich, G.V., and Baranski, T.J. (2006) Genetic analysis of the first and third extracellular loops of the C5a receptor reveals an essential WXFG motif in the first loop. *J. Biol. Chem.* **281**, 12010–12019
10. Minic, J., Sautel, M., Salesse, R., and Pajot-Augy, E. (2005) Yeast system as a screening tool for pharmacological assessment of G protein coupled receptors. *Curr. Med. Chem.* **12**, 961–969
11. Scarselli, M., Li, B., Kim, S.K., and Wess, J. (2007) Multiple residues in the second extracellular loop are critical for M_3 muscarinic acetylcholine receptor activation. *J. Biol. Chem.* **282**, 7385–7396
12. Yellen, G. and Migeon, J.C. (1990) Expression of Torpedo nicotinic acetylcholine receptor subunits in yeast is enhanced by use of yeast signal sequences. *Gene* **86**, 145–152
13. Tanino, T., Matsumoto, T., Fukuda, H., and Kondo, A. (2004) Construction of system for localization of target protein in yeast periplasm using invertase. *J. Mol. Catal. B: Enzymatic* **28**, 259–264
14. Yamada, R., Bito, Y., Adachi, T., Tanaka, T., Ogino, C., Fukuda, H., and Kondo, A. (2009) Efficient production of ethanol from raw starch by a mated diploid *Saccharomyces cerevisiae* with integrated α-amylase and glucoamylase genes. *Enzyme & Microbial. Technol.* **44**, 344–349
15. King, K., Dohlman, H.G., Thorner, J., Caron, M.G., and Lefkowitz, R.J. (1990) Control of yeast mating signal transduction by a mammalian β_2-adrenergic receptor and G_s α subunit. *Science* **250**, 121–123
16. Sander, P., Grunewald, S., Bach, M., Haase, W., Reilander, H., and Michel, H. (1994) Heterologous expression of the human D_{2S} dopamine receptor in protease-deficient *Saccharomyces cerevisiae* strains. *Eur. J. Biochem.* **226**, 697–705
17. Akada, R., Kitagawa, T., Kaneko, S., Toyonaga, D., Ito, S., Kakihara, Y., Hoshida, H., Morimura, S., Kondo, A., and Kida, K. (2006) PCR-mediated seamless gene deletion and marker recycling in *Saccharomyces cerevisiae*. *Yeast* **23**, 399–405
18. Gietz, D., St Jean, A., Woods, R.A., and Schiestl, R.H. (1992) Improved method for high efficiency transformation of intact yeast cells. *Nucleic Acids Res.* **20**, 1425
19. Brown, A.J., Dyos, S.L., Whiteway, M.S., White, J.H., Watson, M.A., Marzioch, M., Clare, J.J., Cousens, D.J., Paddon, C., Plumpton, C., Romanos, M.A., and Dowell, S.J. (2000) Functional coupling of mammalian receptors to the yeast mating pathway using novel yeast/mammalian G protein α-subunit chimeras. *Yeast* **16**, 11–22
20. Overton, M.C. and Blumer, K.J. (2002) The extracellular N-terminal domain and transmembrane domains 1 and 2 mediate oligomerization of a yeast G protein-coupled receptor. *J. Biol. Chem.* **277**, 41463–41472
21. Milligan, G. (2009) G protein-coupled receptor hetero-dimerization: contribution to pharmacology and function. *Br. J. Pharmacol.* **158**, 5–14
22. Watt, H.L., Kharmate, G.D., and Kumar, U. (2009) Somatostatin receptors 1 and 5 heterodimerize with epidermal growth factor receptor: agonist-dependent modulation of the downstream MAPK signalling pathway in breast cancer cells. *Cell Signal.* **21**, 428–439
23. Stroh, T., Jackson, A.C., Sarret, P., Dal Farra, C., Vincent, J.P., Kreienkamp, H.J., Mazella, J., and Beaudet, A. (2000) Intracellular dynamics of sst_5 receptors in transfected COS-7 cells: maintenance of cell surface receptors during ligand-induced endocytosis. *Endocrinology* **141**, 354–365
24. Brachmann, C.B., Davies, A., Cost, G.J., Caputo, E., Li, J., Hieter, P., and Boeke, J.D. (1998) Designer deletion strains derived from *Saccharomyces cerevisiae* S288C: a useful set of strains and plasmids for PCR-mediated gene disruption and other applications. *Yeast* **14**, 115–132
25. Winzeler, E.A., Shoemaker, D.D., Astromoff, A., Liang, H., Anderson, K., Andre, B., Bangham, R., Benito, R., Boeke, J.D., Bussey, H., Chu, A.M., Connelly, C., Davis,

K., Dietrich, F., Dow, S.W., El Bakkoury, M., Foury, F., Friend, S.H., Gentalen, E., Giaever, G., Hegemann, J.H., Jones, T., Laub, M., Liao, H., Liebundguth, N., Lockhart, D.J., Lucau-Danila, A., Lussier, M., M'Rabet, N., Menard, P., Mittmann, M., Pai, C., Rebischung, C., Revuelta, J.L., Riles, L., Roberts, C.J., Ross-MacDonald, P., Scherens, B., Snyder, M., Sookhai-Mahadeo, S., Storms, R.K., Veronneau, S., Voet, M., Volckaert, G., Ward, T.R., Wysocki, R., Yen, G.S., Yu, K., Zimmermann, K., Philippsen, P., Johnston, M., and Davis, R.W. (1999) Functional characterization of the *S. cerevisiae* genome by gene deletion and parallel analysis. *Science* **285**, 901–906

26. Sato, N., Matsumoto, T., Ueda, M., Tanaka, A., Fukuda, H., and Kondo, A. (2002) Long anchor using Flo1 protein enhances reactivity of cell surface-displayed glucoamylase to polymer substrates. *Appl. Microbiol. Biotechnol.* **60**, 469–474
27. Ishii, J., Tanaka, T., Matsumura, S., Tatematsu, K., Kuroda, S., Ogino, C., Fukuda, H., and Kondo, A. (2008) Yeast-based fluorescence reporter assay of G protein-coupled receptor signalling for flow cytometric screening: *FAR1*-disruption recovers loss of episomal plasmid caused by signalling in yeast. *J. Biochem.* **143**, 667–674
28. Ishii, J., Izawa, K., Matsumura, S., Wakamura, K., Tanino, T., Tanaka, T., Ogino, C., Fukuda, H., and Kondo, A. (2009) A simple and immediate method for simultaneously evaluating expression level and plasmid maintenance in yeast. *J. Biochem.* **145**, 701–708

Published online 2 December 2009

Nucleic Acids Research, 2010, Vol. 38, No. 4 e21
doi:10.1093/nar/gkp1101

Selection of DNA aptamers using atomic force microscopy

Yusuke Miyachi[1], Nobuaki Shimizu[2], Chiaki Ogino[1,*] and Akihiko Kondo[1]

[1]Department of Chemical Science and Engineering Faculty of Engineering, Graduate School of Engineering, Kobe University, Rokkoudai-chou 1-1, Nada, Kobe 657-8501 and [2]Division of Material Sciences, Graduate School of Natural Science and Technology, Kanazawa University, Japan

Received August 10, 2009; Revised October 23, 2009; Accepted November 9, 2009

ABSTRACT

Atomic force microscopy (AFM) can detect the adhesion or affinity force between a sample surface and cantilever, dynamically. This feature is useful as a method for the selection of aptamers that bind to their targets with very high affinity. Therefore, we propose the Systematic Evolution of Ligands by an EXponential enrichment (SELEX) method using AFM to obtain aptamers that have a strong affinity for target molecules. In this study, thrombin was chosen as the target molecule, and an 'AFM-SELEX' cycle was performed. As a result, selected cycles were completed with only three rounds, and many of the obtained aptamers had a higher affinity to thrombin than the conventional thrombin aptamer. Moreover, one type of obtained aptamer had a high affinity to thrombin as well as the anti-thrombin antibody. AFM-SELEX is, therefore, considered to be an available method for the selection of DNA aptamers that have a high affinity for their target molecules.

INTRODUCTION

Aptamers are rare functional nucleic acid motifs derived from libraries of nucleic acids by iterative rounds of selection and amplification using a process called Systematic Evolution of Ligands by EXponential enrichment (SELEX) (1–5). In the aptamer selection process, the oligonucleotide library is incubated with a target of interest and a buffer of choice at a given temperature. The bound oligonucleotides are then separated from the unbound oligonucleotides, either by filtration on nitrocellulose filters or by affinity processes such as covalent binding to a titer plate or streptavidin (SA)-coated beads. Aptamers have been selected for a wide variety of targets—for example, low-molecular compounds such as ethanolamine ATP (5–13) and proteins (14–17). Importantly, the isolated aptamers often show high specificity and affinity to their cognate targets. These properties expand the possible applications of aptamers, including their use in diagnosis (13,18–20), therapy and imaging processes (21,22).

Previously reported methods for aptamer selection have included affinity chromatography separation step (14–17). The successful selection of high-affinity aptamers from a library of nucleic acids depends mainly on the efficiency with which the unbound species can be separated from the bound sequences. In many cases, however, DNA aptamers selected by conventional SELEX strategy for adenosine triphosphate (K_D: 1×10^{-6} order), hematoporphyrin (K_D: 1×10^{-4} to 1×10^{-6}) and thrombin (K_D: 1×10^{-7} order), have a low affinity (7–17). Since the dissociation constant of antibody, often used for biosensing device, had been reported to be 1×10^{-8} to 1×10^{-10} M, the affinities of these reported DNA aptamers were weaker than that of antibody to antigen (23–27). When DNA aptamers are used with biosensing devices, a low affinity to the target molecule will result in unreliable results for detection sensitivity.

Atomic force microscopy (AFM) is a method that scans the imperceptible sample surface using a probe called a cantilever, detecting the weak force between sample surface and probe, and makes pictures of the sample surface. AFM can also dynamically detect the adhesion or affinity force between the sample surface and the cantilever (21,22,28,29). This notable feature is useful for measurement of the affinity force of biomolecule interactions using the biomolecule immobilized cantilever and the sample. This system is considered to be a selection method for aptamers. Therefore, we propose the SELEX method using AFM to obtain aptamers having a strong affinity to target molecules.

The selection scheme of this SELEX strategy is shown in Figure 1. DNA aptamers with a very strong affinity to target molecules were obtained by repeating this cycle. In this study, thrombin was chosen as the target molecule of the DNA aptamer, and the selection cycles were repeated for three rounds. As a result, the obtained DNA aptamers had a high affinity to thrombin than that

*To whom correspondence should be addressed. Tel/Fax: +81 78 803 6193; Email: ochiaki@port.kobe-u.ac.jp

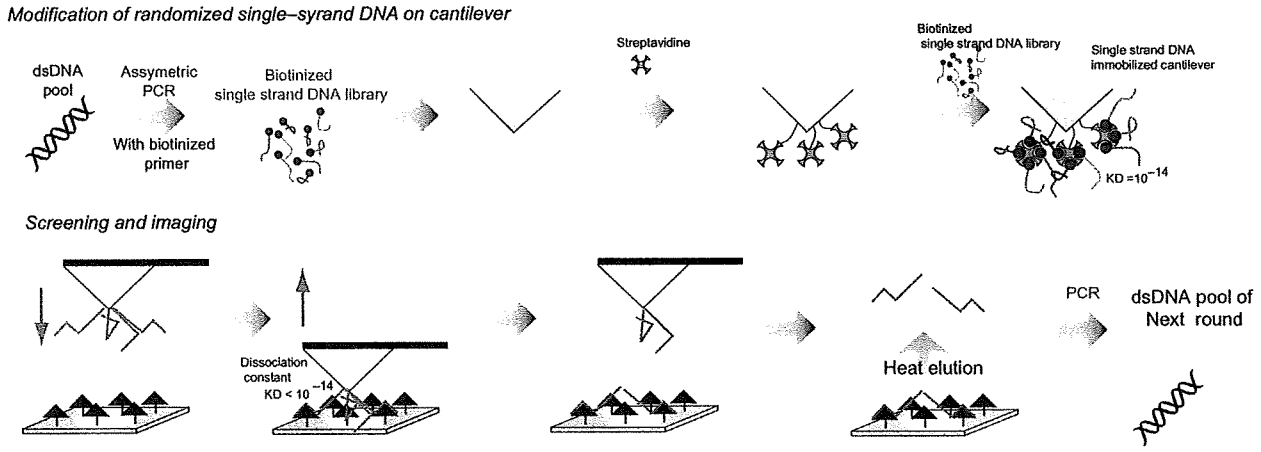

Figure 1. The scheme of a new SELEX strategy for functional oligonucleotide screening by AFM.

of conventional thrombin aptamer. One type of DNA aptamer exhibited high affinity as well as that of an antibody.

MATERIALS AND METHODS

Materials

Thrombin from human plasma and streptavidin from *Streptomyces avidinii* were purchased from Sigma (MO, USA). Anti-human thrombin antibody from sheep was purchased from Funakoshi (Tokyo, Japan). DNA polymerase was purchased from Roche Diagnostics (Basel, Switzerland). A microspin column was purchased from GE Healthcare (MO, USA). 3,3′-Dithiobis [sulfosuccinimidylpropionate] (DTSSP) was purchased from Pierce (MO, USA). The other chemicals used were analytical grade and were purchased from Nacalai Tesque (Kyoto, Japan).

Preparation of the cantilever as modified by single-strand DNA (ssDNA) library

In the primary round, for double-strand DNA library (dsDNA) production, a synthetic DNA oligonucleotide library (104-mer) with 60 random nucleotide sequences, 5′-TAGGGAATTCGTCGACGGATCC-N60-CTGCAG GTCGACGCATGCGCCG-3′, was amplified over 25 cycles of PCR (95°C, 15 s; 72°C, 30 s) using the following pair of primers: 5′-TAATACGACTCACTATAGGGAA TTCGTCGACGGAT-3′ (P1) and 5′-CGGCGCATGCG TCGACCTG-3′ (P2). The ssDNA library was then obtained from the dsDNA by an additional 90 cycles of asymmetric PCR using 5′ biothinated P1 primer. The PCR product, ssDNA, was purified by microspin column.

To clear away the organic compounds that adhered on the cantilever, the cantilever was treated with UV for 2 h. The probe was then exposed to 100 µl of 2 mg/ml DTSSP solution in 20 mM acetate (pH 4.8) at room temperature for 30 min. After the reaction, the probe was dipped in 20 ml of ultra pure water to remove unreacted DTSSP. The succinimide immobilized probe was then doused at room temperature for 1 h with 100 µl of 1 mg/ml streptavidin solution in PBS, followed by washing with 20 ml of folding buffer. After immobilization of streptavidin on the cantilever, 100 µl of 5 µM biothinated ssDNA was dropped on the cantilever and incubated at room temperature for 30 min. Finally, the ssDNA immobilized probe was put in 20 ml of folding buffer containing 0.01% Tween 20 to remove unbound biothinated ssDNA.

Preparation of gold chip modified by thrombin

A gold chip was covered by 200 µl of 4 mg/ml DTSSP solution in 20 mM acetate at room temperature for 30 min. The chip was then washed with 10 ml of ultra pure water. After washing, the succinimide immobilized gold chip was covered with 200 µl of 6 µg/ml thrombin solution in PBS at room temperature for 1 h. Finally, the gold chip was washed with 10 ml of folding buffer.

SELEX strategy based on AFM

Force curve mapping was performed in the liquid cell of a SPA400-Nanonavi AFM unit (SII Nanotechnology Inc., Chiba, Japan) with the cantilever and gold chip described above. The force curve measurements were performed in folding buffer [50 mM Tris–HCl (pH 7.6), 300 mM NaCl, 30 mM KCl and 5 mM $MgCl_2$]. Force curves were recorded at a velocity of 17 µm/s. Topographic images were captured at 64 × 64 pixels resolution with a scan size of 1 µm × 1 µm. The adhesion forces analysis between ssDNA immobilized on tip of cantilever and thrombin were measured at 4096 data points (64 × 64 point), and a histogram of these adhesion force was charted. According to the AFM-SELEX, scanning was carried out five times (4096 × 5 times) in round 1 and 2, and 4 times (4096 × 4 times) in round 3, respectively.

After the scanning and force curve mapping, the ssDNA-bound gold chip was washed with 10 ml folding

buffer containing 0.01% Tween 20. Then, to elute ssDNA on the gold chip, the chip was dunked in 2 ml of 20 mM TE buffer containing 1% DMSO and incubated at 98°C for 10 min and on ice for 10 min. The eluted ssDNAs were precipitated by ethanol, dissolved in 100 µl of 20 mM TE buffer, and used for the next selection as a PCR template.

Cloning and sequencing

The dsDNAs obtained after the fourth rounds of selection were subcloned into pT7 blue vector, and then transformed into *Escherichia coli* (Nova blue). The plasmid DNA was isolated by the alkaline-extraction method. Twenty-two colonies were randomly selected after the fourth round, and these DNA sequences were determined by a dye-terminator method using CEQ 8000 (Beckman).

Affinity assay of obtained aptamers by AFM

For dsDNA production, obtained DNA was amplified over 15 cycles of PCR (95°C, 15 s; 72°C, 30 s) using P1 and P2 primer. The ssDNA was then obtained from the dsDNA by an additional 90 cycles of asymmetric PCR using 5′ biothinated P1 primer. The PCR product, ssDNA, was purified by microspin column.

The preparation of the cantilever immobilizing ssDNA and the gold chip immobilizing thrombin was followed by selection methods. The affinity force of the conventional thrombin aptamer and antibody to thrombin was analyzed as a positive control under the same conditions.

Fluorescence polarization measurement

The dissociation constant of TBA-1 was calculated by fluorescence polarization. Each of various concentrations of thrombin and FITC labeled TBA-1 (final concentration: 100 nM) was mixed in the folding buffer for 2 h, and fluorescence polarization measurement was carried out (EnVision, Perkin elmer, Wellesley, MA). As a negative control of thrombin, 100 nM streptavidin was used, and fluorescence polarization measurement was carried out under same condition. Each data was represented three independent experimental data, and each error bar was mean of standard deviation.

RESULTS

Selection of DNA aptamer using AFM

At first, the biotinated random ssDNA was immobilized on the cantilever through avidin, and the target molecules were immobilized on the gold chip. The prepared cantilever and gold chip were simultaneously applied to AFM as a DNA-modified probe and thrombin immobilized chip, respectively. When the cantilever approached the gold chip, the DNA aptamer that binds the target molecules would bind the target immobilized on the gold chip. If the affinity force with target is very strong, the avidin-biotin interaction is fractured, and DNA aptamer remains on the gold chip. The remaining DNA was recovered by heat elution amplified by PCR.

The selection cycle by AFM-SELEX was repeated for three rounds. The histogram of the affinity force between ssDNA and thrombin was developed from 4096 force curves from each round (Figure 2A–D). As a result, the affinity force between ssDNA and thrombin was gradually increased with repeated selection rounds. The initial ssDNA and round 1 elution pool had low affinity force to thrombin (Figure 2A and B). However, in the round 2 elution pool the force was higher, over 100 pN, and in the round 3 elution pool the histogram of affinity force had a peak at 320–329 pN. Using the histogram data, the average affinity force of each round was calculated (Figure 2E). The average force of the initial pool was ~57.15 pN (Figure 2A and E). However, after only three repeated rounds of the AFM-SELEX method, the ssDNA pool had 411.52 pN of strong affinity to thrombin (Figure 2D and E).

In Figure 3, the topography of the affinity force between the round 3 elution pool and thrombin is shown. The highest point of affinity force was concentrated late in the scanning (Figure 3A). Moreover, the force had no relationship with the roughness of the sample, since the higher force was not operating at the height of the surface roughness.

Cloning and sequencing

The dsDNAs obtained after the third round of selection were subcloned into pT7 blue vector. Twenty-two colonies were randomly selected, and these DNA sequences were determined (Table 1). Many of the obtained DNAs had G-rich sequences. The sequence called TBA-1 had the largest share of obtained aptamers. Moreover, the sequences of TBA-1 and -2 had many 'GGGGT' motifs.

Binding assay using AFM

The immobilization method described above was followed by the SELEX protocol. The prepared cantilever and gold chip were applied to AFM to analyze the affinity force between ssDNA and thrombin. The resulting force histogram of TBA-1 had one peak at 210-219 pN (Figure 4A). The histogram of TBA-2 had two peaks at 40–49 and 110–119 (Figure 4B). The average affinity force between thrombin and the obtained aptamers was calculated. The obtained aptamers had a higher affinity for thrombin than N60 ssDNA and the conventional thrombin aptamer (Figure 4C and Table 2). TBA-1 had the highest affinity of the obtained DNA aptamers. The affinity force of the conventional DNA aptamer that has the 'GGTTGGTGT GGTTGG' sequence was also measured by AFM, and the resulting force average was 65.09 pN. The average affinity force was 205.52 pN, and the value was about three times higher than that of the conventional thrombin aptamer. The affinity force between anti-thrombin antibody and thrombin was then analyzed by AFM. The resulting average affinity force was 91.59 pN (Figure 4D and Table 2).

Fluorescence polarization measurement

The fluorescence polarization measurement between TBA-1 and thrombin was carried out, and the recognition affinity obtained by AFM analysis was re-confirmed.

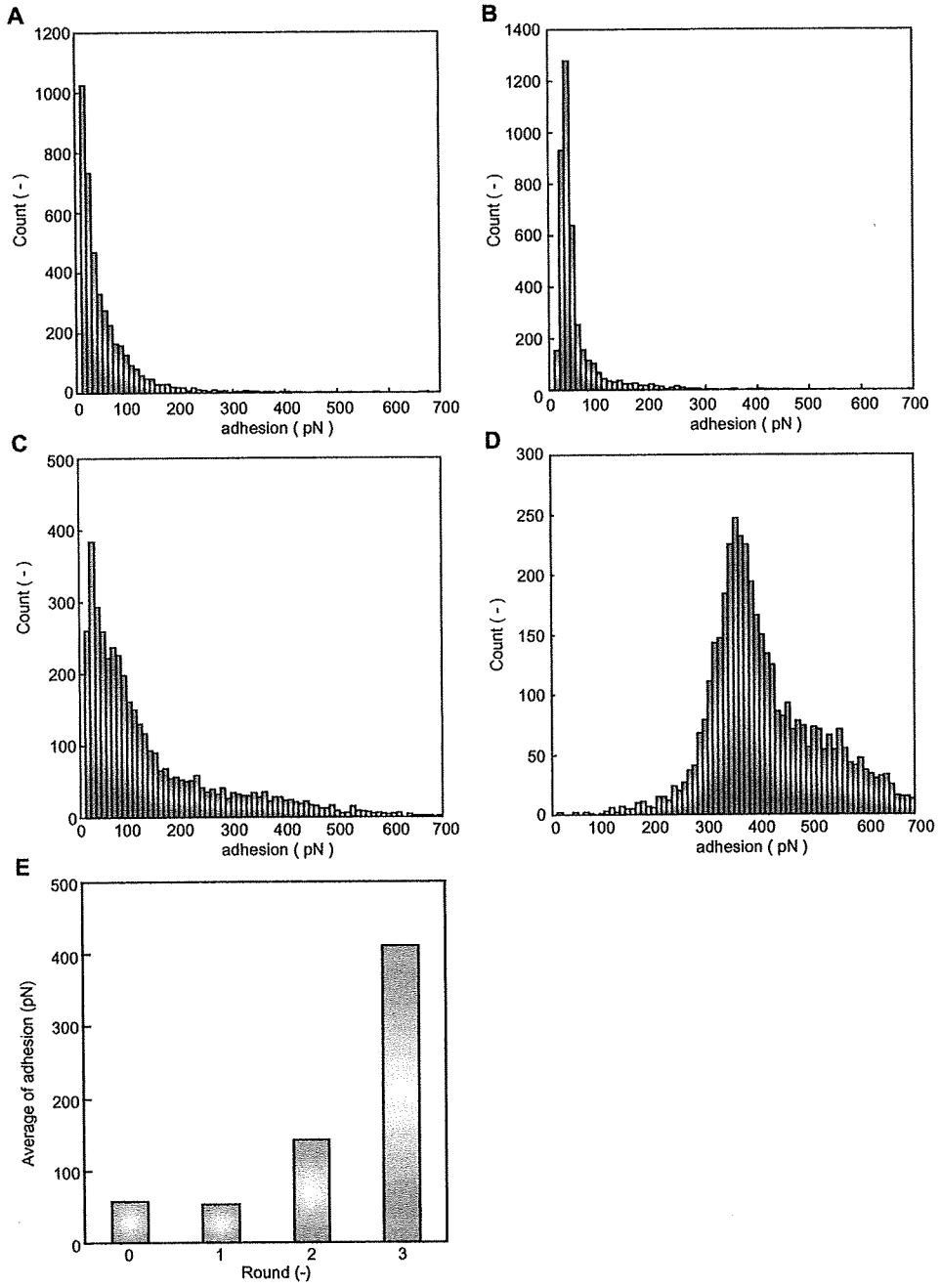

Figure 2. Histogram of adhesion force between ssDNA and protein for 4096 data points. (**A**) adhesion force between 0 pool ssDNA and thrombin, (**B**) adhesion force between round 1 elution pool and thrombin, (**C**) adhesion force between round 2 elution pool and thrombin, (**D**) adhesion force between round 3 elution pool and thrombin and (**E**) the average of affinity force between each round elution pool and thrombin.

The concentration of thrombin was changed from 10^{-13}–10^{-7} M, and then polarization value was plotted against the concentration of thrombin (Figure 5). As a result, the fluorescence polarization value was increased with concentration dependency. On the other hand, polarization value of FITC-labeled TBA-1 against with 100 nM streptavidin was not increased significantly (Table 3).

DISCUSSION

SELEX strategy using AFM

The selection of a DNA aptamer with AFM was performed using 60 random nucleotide sequences. After the first SELEX round, dsDNA was not amplified enough by 15 PCR cycles, since the amount of elution DNA was very

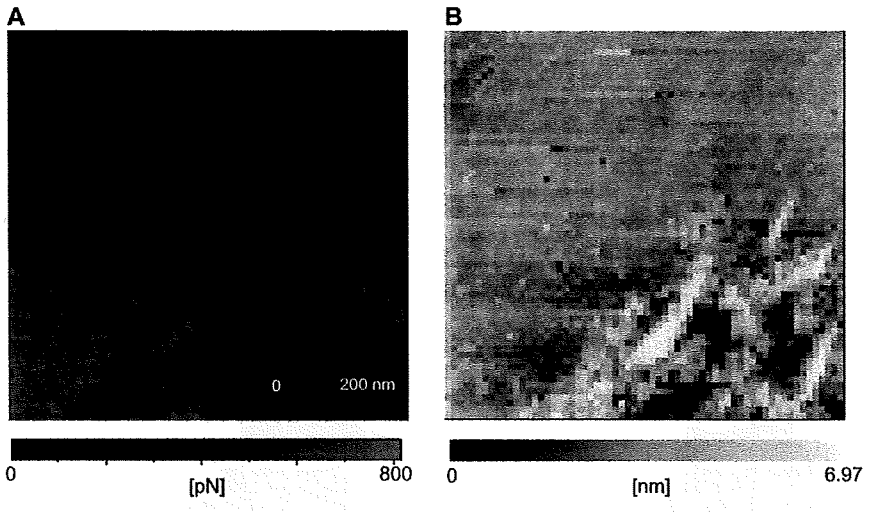

Figure 3. Affinity image between round 3 elution pool and thrombin showing the affinity images (A) as well as the topography images (B).

Table 1. Sequence of obtained single-strand DNA

Sequence name	Sequence of random region	Count
TBA1	CCTAGTGTGCGTCGATGGGGTGGGGTGGGGCTGAGTTGGGGGGTGGGATCAATCAATCTGGTTT	8
TBA2	CCTAGTGTGCGTCGATGGGGTGGGGTGGGGCTGAGTTGGGGGGTGGGATCAATCCATCTGGTCT	2
The other 1	CCCACGGAGTCACCATTGATCACAACCCCAGCT	1
The other 2	CCCACGGAGCCACCACCTTGATCACAACCCTCAGCT	1
The other 3	CCCACGGAGTCACCCTTGATCACAACCTCAGCT	2
The other 4	CCCACGGAGTCACCCTTGACCACAATCTCAGCT	1
The other 5	CCCACGGAGCCACCCTTGATCACAGCCTCAGCT	1
The other 6	CCCACGGAGTCACCCTTGATCACGAACCTCAGCT	1

small (data not shown). However, after the third SELEX round, the amount of dsDNA amplified by PCR was determined by PAGE to be large. Based on these results, selection by the AFM-SELEX strategy appeared to be very strong, and the ssDNA that binded strongly to thrombin was selected.

The selection cycle was repeated for three rounds. Figure 2 shows the histogram of adhesion force between ssDNA and thrombin. The initial ssDNA pool had a low adhesion force to thrombin, since the ssDNA had a low affinity for thrombin (Figure 2A). However, when the AFM-SELEX method was repeated for three rounds, the ssDNA had a strong affinity for thrombin (Figure 2D). Moreover, the third round elution pool did not have a large adhesion force to streptavidin, ~67.14 pN (data not shown). This result shows that the third round elution pool bound specifically to thrombin. The affinity force between ssDNA and thrombin then gradually became stronger with repeated selection rounds (Figure 2E). Therefore, it is considered that ssDNA had an affinity for thrombin and was enriched by the repeating of the AFM-SELEX cycles.

In many articles on DNA aptamer, the selection cycle is repeated for more than eight rounds (8–12). However, in the selection method with AFM, the DNA aptamer with a high affinity for the target molecules was obtained by repeating only three rounds. Therefore, the AFM-SELEX strategy is a very useful method to rapidly obtain a DNA aptamer. In this new SELEX strategy using AFM, the oligonucleotide that could be bound to thrombin was only remained on gold chip. Therefore, compared with conventional SELEX strategy, it is considered that the non-specific bound of DNA was assumed to be reduced on gold chip surface, and the DNA aptamer that have high affinity to thrombin could be rapidly obtained.

The topography between round 3-elution pool and thrombin was analyzed (Figure 3B). In commonly, at the point of large roughness, the large force was occurred because of impact between cantilever and surface roughness. However, the high affinity forces, caused by molecular interaction between selected DNA aptamers and thrombin, were observed in every place, and this phenomenon was not related to the result of topology analysis (Figure 3A). Together these results, it was concluded that the specific affinity originated by molecular interaction was not related on surface roughness, and the specific adhesion force by affinity between round-3-elution pool and

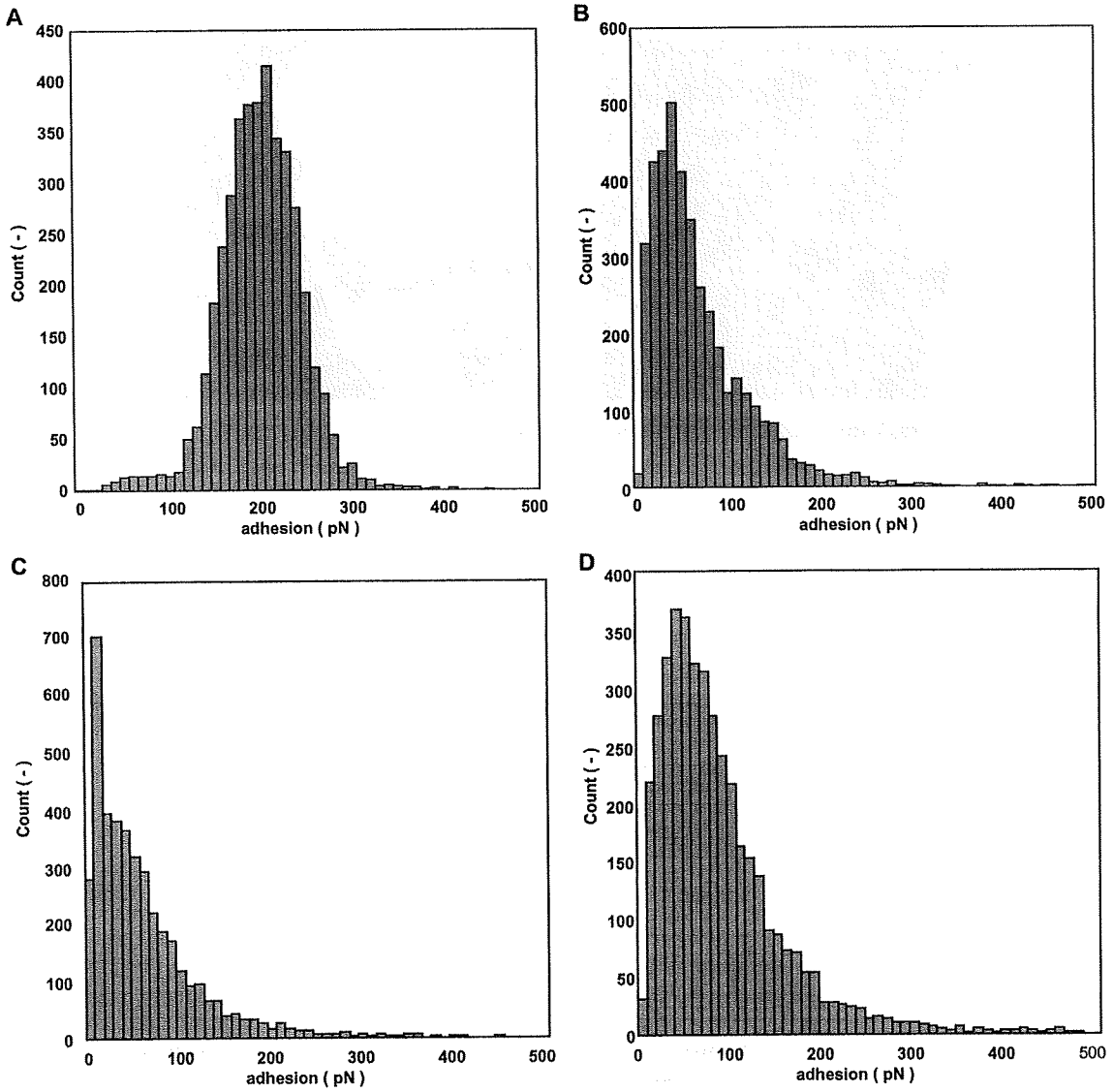

Figure 4. Histogram of the affinity force between aptamer and thrombin for 4096 data points. (**A**) TBA-1, (**B**) TBA-2, (**C**) conventional thrombin aptamer and (**D**) anti-thrombin antibody.

Table 2. The average of affinity force between obtained aptamer and thrombin

	Average of affinity force (pN) (mean ± SE)	Peak position (pN)
N60	57.15 ± 0.96	10–19
TBA-1	205.52 ± 0.70	210–219
TBA-2	74.48 ± 0.90	40–49, 110–119
Conventional thrombin aptamer	65.09 ± 0.98	10–19
Anti-thrombin antibody	91.59 ± 1.09	50–59

thrombin could be measured. Furthermore, the SELEX cycle number was suitable with three round since the affinity of TBA-1 to thrombin is significantly larger than that of anti-thrombin antibody at three rounds.

Sequence analysis

The third-round elution DNA that suggested the strongest binding to thrombin was subcloned to pT7 blue vector, and the sequence was determined. Many of the resultant obtained DNA sequences had a G-rich sequence (Table 1). Previously, thrombin aptamer possessing a G-rich sequence had been reported (14). According to this previous reported result, thus, it was assumed that the oligonucleotide sequence called TBA-1 could be functioned as a DNA aptamer against with thrombin.

Binding assay and determination of dissociation constant

The histogram of the affinity force between obtained aptamers called TBA-1 and -2 and thrombin was depicted from 4096 points of force curves (Figure 4A

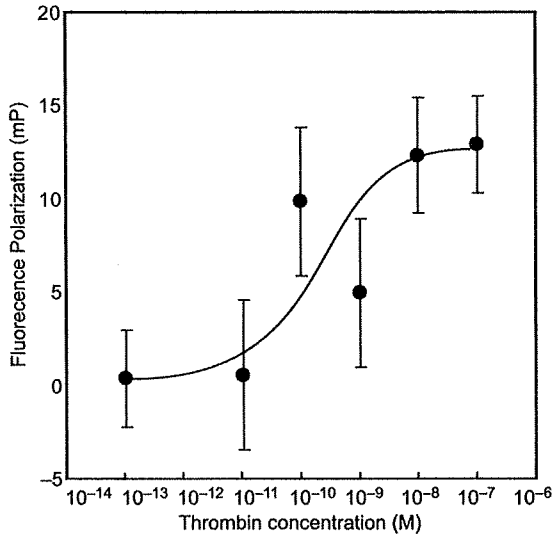

Figure 5. Binding curve of TBA-1 with thrombin. Each of thrombin solution (10^{-7}–10^{-13} M) was mixed with TBA-1 (100 nM), and incubated for 2 h at room temperature. After incubation, the polarization was measured.

Table 3. The fluorescence polarization value between TBA-1 and thrombin or streptavidin

	Polarization value (mP)	SE
Thrombin	12.9	2.60
Avidin	0.23	3.25

and B). The force histogram of TBA-1 had one peak at 210–219 pN (Figure 4A). These results suggest that there is a single binding site of TBA-1 to thrombin. On the other hand, the histogram of TBA-2 has three peaks at 40–49 and 110–119 pN (Figure 4B). The force value of the second peak is twice as large as that of the first peak. For these reasons, TBA-2 is considered to have two binding sites to thrombin.

The average affinity force between aptamer and thrombin was calculated from 4096 point force curve data (Table 2). The force average of TBA-1 was 203.52 pN, and the affinity of the N60 pool to thrombin was 57.14 pN. These results indicate that obtained ssDNAs have a high affinity to thrombin.

On the other hand, the conventional thrombin aptamers that have the 'GGTTGGTGTGGTTGG' sequence have the affinity force of 65.09 pN (Figure 4C and Table 2). Therefore, the affinity of obtained DNA aptamers to thrombin is stronger than that of the conventional thrombin aptamer. In previously report, the average of affinity force between conventional selected thrombin aptamer and thrombin is 4.45 pN. However, in this study, the affinity force was estimated to be 65.09 pN. It was considered that this difference was depended on the immobilization method and the DNA aptamer molecule number involved in immobilization. In addition, the affinity force between anti-thrombin antibody and thrombin is 91.59 pN (Figure 4D and Table 2). Therefore, the affinity of the TBA-1 aptamer to thrombin is stronger than that of antibody to thrombin.

For determination of dissociation constant (K_D), the fluorescence polarization analysis was carried out. As a result, binding curve was increased with thrombin concentration dependency (Figure 5). However, in the case of streptavidin, the polarization value of FITC-labeled TBA-1 was not increased significantly (Table 3). Therefore, it is considered that the binding affinity of TBA to thrombin is specifically. By fluorescence polarization analysis, the K_D value of TBA-1 against thrombin is estimated to be 200 pM (2×10^{-10} M). Although K_D value of streptavidin–biotin interaction was 1×10^{-14} order, however, as a result, the binding affinity of TBA-1 to thrombin is 10 000-fold lower than that of streptavisdin–biotin interaction. Generally, free streptavidin exhibited a high affinity interaction described above. However, in the case of immobilized streptavidin, the K_D value to biothin was decreased to 1×10^{-8} to 1×10^{-10} M order by conformation alternation (30). In AFM SELEX analysis, the streptavidin was covalently immobilized on the tip of surface of cantilever. Therefore, it was considered that K_D value of streptavidin was decreased by immobilization, and as a result, the DNA aptamers with comparable lower affinity were selected.

As mentioned above, the K_D value of isolated DNA aptamer TBA-1 was 1000 times lower than conventional aptamer having 200 nM of dissociation constant to thrombin (14). Moreover, this result was strongly supported to AFM analysis of TBA-1 affinity. Moreover, by AFM analysis, there was significant difference between the affinity of TBA-1 and the affinity of antibody to thrombin, and affinity force of TBA-1 was strongly compared with that of anti-thrombin antibody. Therefore, it was considered that the dissociation constant of TBA-1 to thrombin is $<10^{-8}$ – 10^{-10} M, since the dissociation constant of antibody to antigen is $\sim 10^{-8}$ –10^{-10} M (23–27). However, there was no significant difference of dissociation constant between TBA-1 and antibody to thrombin. Therefore, it was considered that TBA-1 was optimized on AFM analysis.

In many reports, the dissociation constant of aptamers to their target molecules is 10 – 0.01 μM, and the aptamers that have low affinity are also selected (7–17). This is because the affinity force of obtained aptamers to their target cannot be controlled when using a conventional SELEX method. This AFM-SELEX strategy permit us to not only selecting quickly, but also obtaining high affinity DNA aptamer to the target as well as that of antibody to antigen. Therefore, this method may have a practical advantage for obtaining aptamers that have a strong affinity to targets.

Concluding remarks

In this study, a DNA aptamer that binds to thrombin with very high affinity and specificity was selected using AFM. The affinity force between ssDNA and thrombin grew gradually stronger upon repeating selection rounds.

In addition, the sequences of obtained aptamers have many G-rich regions. One type of obtained aptamers, called TBA-1, has a strong affinity to thrombin compared with the conventional thrombin aptamer. This result suggests that DNA aptamers that bind to their targets with high affinity can be selected by AFM-SELEX. In addition, it suggests that DNA aptamers could be selected using fewer rounds, as compared with a conventional SELEX strategy. Considered together, these results indicate that this new SELEX strategy could be a viable candidate for the screening for various DNA aptamers with high affinities.

FUNDING

Funding for open access charge: Grant-in-Aid from the Ministry of Education, Culture, Sports, Science and Technology, Japan (No. 19021017 to C.O.), the foundation from New Energy and Industrial Technology Development Organization (NEDO) of Japan (No. 06B44019 to C.O.) and the Special Coordination Funds for Promoting Science and Technology, Creation of Innovation Centers for Advanced Interdisciplinary Research Areas (Innovative Bioproduction Kobe), MEXT, Japan.

Conflict of interest statement. None declared.

REFERENCES

1. Bass,L. and Cech,R. (1984) Specific interaction between the self-splicing RNA of Tetrahymena and its guanosine substrate: implications for biological catalysis by RNA. *Nature*, **308**, 820–826.
2. Gold,L., Polisky,B., Uhlenbeck,O. and Yarus,M. (1995) Diversity of oligonucleotide functions. *Annu. Rev. Biochem.*, **64**, 763–797.
3. Osborne,S. and Ellington,A. (1997) Nucleic acid selection and the challenge of combinatorial chemistry. *Chem. Rev.*, **97**, 349–370.
4. Wilson,D.S. and Szostak,Z. (1999) In vitro selection of functional nucleic acids. *Annu. Rev. Biochem.*, **68**, 647–661.
5. Misono,T.S. and Kumar,K.R. (2005) Selection of RNA aptamers against human influenza virus hemagglutinin using surface plasmon resonance. *Anal. Biochem.*, **342**, 312–317.
6. Davis,J.H. and Szostak,J.W. (2002) Isolation of high-affinity GTP aptamers from partially structured RNA libraries. *Proc. Natl Acad. Sci. USA*, **99**, 11616–11621.
7. Tuerk,C. and Gold,L. (1990) Systematic evolution of ligands by exponential enrichment: RNA ligands to bacteriophage T4 DNA polymerase. *Science*, **249**, 505–510.
8. Huuizengen,D.E. and Szostak,J.W. (1995) A DNA aptamer that's binds adenosine and ATP. *Biochemistry*, **34**, 656–665.
9. Miyachi,Y., Shimizu,N., Ogino,C., Fukuda,H. and Kondo,A. (2009) Selection of a DNA aptamer that binds 8-OHdG using GMP-agarose. *Bioorg. Med. Chem. Lett.*, **19**, 3619–3622.
10. Okazawa,A., Maeda,H., Fukusaki,E., Katakura,Y. and Kobayashi,A. (2000) In vitro selection of hematoporphyrin binding DNA aptamers. *Bioorg. Med. Chem. Lett.*, **10**, 2653–2656.
11. Niazi,J.H., Lee,S.J., Kim,Y.S. and Gu,M.B. (2008) ssDNA aptamers that selectively bind oxytetracycline. *Bioorg. Med. Chem.*, **16**, 1254–1261.
12. Mann,D., Reinemann,C., Stoltenburg,R. and Strehlitz,B. (2005) In vitro selection of DNA aptamers binding ethanolamine. *Biochem. Biophys. Res. Commun.*, **338**, 1928–1934.
13. Kima,Y.S., Jung,H.S., Matsuura,T., Lee,H.Y., Kawai,T. and Gua,M.B. (2007) Electrochemical detection of 17β-estradiol using DNA aptamer immobilized gold electrode chip. *Biosens. Bioelectron.*, **22**, 2525–2531.
14. Bock,L., Griffin,L., Latham,J., Vernaas,E. and Toole,J. (1992) Selection of single-strand DNA molecules that bind and inhibit human thrombin. *Nature*, **355**, 564–566.
15. Hasegawa,H., Sode,K. and Ikebukuro,K. (2008) Selection of DNA aptamers against VEGF165 using a protein competitor and the aptamer blotting method. *Biotechnol. Lett.*, **30**, 829–834.
16. Ogasawara,D., Hasegawa,H., Kaneko,K., Sode,K. and Ikebukuro,K. (2007) Screening of DNA aptamer against mouse prion protein by competitive selection. *Prion*, **1**, 248–254.
17. Tang,J., Yu,T., Guo,L., Xie,J., Shao,N. and He,Z. (2007) In vitro selection of DNA aptamer against abrin toxin and aptamer-based abrin direct detection. *Biosens. Bioelectron.*, **22**, 2456–2463.
18. Guthrie,J.W., Hamula,L.A., Zhang,H. and Le,X.C. (2006) Assays for cytokines using aptamers. *Methods*, **38**, 324–330.
19. Ikebukuro,K., Yoshida,W. and Sode,K. (2008) Aptameric enzyme subunit for homogeneous DNA sensing. *Biotechnol. Lett.*, **30**, 243–252.
20. Bini,A., Minunni,M., Tombelli,S., Centi,S. and Mascini,M. (2007) Analytical performances of aptamer-based sensing for thrombin detection. *Anal. Chem.*, **79**, 3016–3019.
21. Basnar,B., Elnathan,R. and Willner,I. (2006) Following aptamer-thrombin binding by force measurements. *Anal. Chem.*, **78**, 3638–3642.
22. Lin,L., Wang,H., Liu,Y., Yan,H. and Lindsay,S. (2006) Recognition imaging with a DNA aptamer. *Biophys. J.*, **90**, 4236–4238.
23. Aixing,D., Weiming,T., Suping,H., Wei,L., Tiegui,N., Zhaohu,L., Baomin,W. and Qing,X. (2008) Monoclonal antibody-based enzyme linked immunosorbent assay for the analysis of Jasmonates in plants. *J. Integr. Plant Biol.*, **50**, 1046–1052.
24. Larvor,M., Ohaniance,L., Nall,B. and Goldberg,M. (1994) Measurement of the dissociation rate constant of antigen/antibody complexes in solution by enzyme-linked immunosorbent assay. *J. Immunol. Methods*, **170**, 167–175.
25. Dill,K., Fraser,C., Blomdahl,J. and Olson,J. (1996) Determination of dissociation constant and concentration of an anti-DNA antibody by using the light-addressable potentiometric sensor. *J. Biochem. Biophys. Methods*, **31**, 17–21.
26. Krämer,P., Gouzy,M., Keß,M., Kleinschmidt,U. and Kremmer,E. (2008) Development and characterization of new rat monoclonal antibodies for procalcitonin. *Anal. Bioanal. Chem.*, **392**, 727–736.
27. Hoylaerts,M., Bollen,A. and De Broe,M. (1990) The application of enzyme kinetics to the determination of dissociation constants for antigen-antibody interactions in solution. *J. Immunol. Methods*, **126**, 253–261.
28. Agnihotri,A., Somana,P. and Siedlecki,C.A. (2009) AFM measurements of interactions between the platelet integrin receptor GPIIbIIIa and fibrinogen. *Colloid Surf. B-Biointerfaces*, **71**, 138–147.
29. Yoshimura,S.H., Takahashi,H., Otsuka,S. and Takeyasu,K. (2006) Development of glutathione-coupled cantilever for the single-molecule force measurement by scanning force microscopy. *FEBS Lett.*, **580**, 3961–3965.
30. Huang,S.C., Stump,M.D., Weiss,R. and Caldwell,K.D. (1996) Binding of biothylated DNA to streptavidin-coated polystyrene latex: effects of chain length and particle size. *Anal. Biochem.*, **237**, 115–122.